

# KECK HIRES Spectroscopy of APM 08279+5255<sup>1</sup>

Sara L. Ellison<sup>2</sup>, Geraint F. Lewis<sup>3</sup>, Max Pettini<sup>2</sup>, Wallace L. W. Sargent<sup>4</sup>, Frederic H. Chaffee<sup>5</sup>, Craig B. Foltz<sup>6</sup>, Michael Rauch<sup>7</sup>, Mike J. Irwin<sup>2</sup>

## ABSTRACT

With an optical  $R$ -band magnitude of 15.2, the recently discovered  $z=3.911$  BAL quasar APM 08279+5255 is an exceptionally bright high redshift source. Its brightness has allowed us to acquire a high signal-to-noise ratio ( $\sim 80$ ), high resolution ( $\sim 6 \text{ km s}^{-1}$ ) spectrum using the HIRES echelle spectrograph on the 10-m Keck I telescope. Given the quality of the data, these observations provide an unprecedented view of associated and intervening absorption systems. Here we announce the availability of this spectrum to the general astronomical community and present a brief analysis of some of its main features.

*Subject headings:* quasars: absorption lines – quasars: individual (APM 08279+5255)

## 1. INTRODUCTION

Discovered serendipitously in a survey of Galactic halo carbon stars, the recently identified  $z=3.911$  BAL quasar APM 08279+5255 (Irwin et al. 1998) possesses an inferred intrinsic

---

<sup>1</sup>The data presented herein were obtained at the W. M. Keck Observatory, which is operated as a scientific partnership among the California Institute of Technology, the University of California and the National Aeronautics and Space Administration. The Observatory was made possible by the generous financial support of the W. M. Keck Foundation.

<sup>2</sup> Institute of Astronomy, Madingley Road, Cambridge CB3 0HA, UK  
Electronic mail contact: [sara@ast.cam.ac.uk](mailto:sara@ast.cam.ac.uk)

<sup>3</sup> Fellow of the Pacific Institute of Mathematical Sciences 1998-1999,  
Dept. of Physics and Astronomy, University of Victoria, PO Box 3055, Victoria, B.C., V8W 3P6, Canada  
& Astronomy Dept., University of Washington, Box 351580, Seattle, WA 98195-1580

<sup>4</sup>Palomar Observatory, Caltech 105-24, Pasadena, CA 91125

<sup>5</sup> W. M. Keck Observatory, 65-1120 Mamalahoa Hwy, Kamuela, HI 96743

<sup>6</sup>MMT Observatory, University of Arizona, Tucson, AZ 85721

<sup>7</sup>European Southern Observatory, Karl-Schwarzschild-Str. 2, D-85748 Garching bei Munchen, Germany.

luminosity of  $\sim 5 \times 10^{15} L_{\odot}$  ( $\Omega_0 = 1, h = 0.5$ ), making it apparently the most luminous system currently known. A significant fraction of this prodigious emission occurs at infrared and sub-mm wavelengths, arising in a massive quantity of warm dust (Lewis et al. 1998). Recent observations have further probed this unusual system; CO observations have demonstrated that APM 08279+5255 also possesses a large quantity of molecular gas (Downes et al. 1999), a reservoir for star formation, while the internal structure of APM 08279+5255 has been probed with polarization studies, indicating that several lines of sight through various absorbing and scattering regions are responsible for the complex polarized spectrum (Hines et al. 1999).

Observations with the 1.0 m Jacobus Kapteyn telescope on La Palma suggest that APM 08279+5255 is not a simple point-like source, but is better represented by a pair of sources separated by  $\sim 0''.4$  (Irwin et al. 1998). This was confirmed with images acquired with the Canada-France-Hawaii AO/Bonnette which revealed two images, separated by  $0''.35 \pm 0''.02$ , with an intensity ratio of  $1.21 \pm 0.25$  (Ledoux et al. 1998); such a configuration is indicative of gravitational lensing and suggests that our view of APM 08279+5255 has been significantly enhanced. More recent NICMOS images have further refined this picture, revealing the presence of a third image between the other two (Ibata et al. 1999). The resulting magnification is by a factor of  $\sim 70$  for the point-like quasar source. However, even when gravitational lensing is taken into account, APM 08279+5255 is still one of the most luminous known QSOs.

We have obtained a high S/N ( $\sim 80$ ), high resolution ( $6 \text{ km s}^{-1}$ ) spectrum of APM 08279+5255, the result of almost 9 hours of observations with HIRES at the Keck I telescope. In this paper we describe some of the most important characteristics of the spectrum and announce its availability to the general astronomical community. In a separate paper (Ellison et al. 1999) we have used these data to throw new light on the question of the C abundance in low column density Ly $\alpha$  forest clouds.

The outline of the paper is as follows. In §2 we describe the observations obtained and the data reduction procedure followed in order to produce the final spectrum. Section 3 presents a brief analysis of some of the absorption systems seen in the QSO spectrum, illustrating the quality and potential of the data. We then, in §4, describe how the data may be obtained from a permanent, anonymous ftp directory in Cambridge<sup>8</sup> before summarising the main results of the paper in §5.

---

<sup>8</sup>Note that as well as the data files available in Cambridge, a full ascii spectrum of APM 08279+5255 is available in the electronic version of this PASP Research Note, together with a complete list of Ly $\alpha$  forest fit parameters—see §3 and Tables 2 and 3

## 2. OBSERVATIONS AND INITIAL REDUCTION

The brightness of APM 08279+5255 presents an excellent opportunity to study spectroscopically the intervening absorption systems and the Broad Absorption Lines intrinsic to the QSO. To this end, a program of high resolution observations was mounted on the 10-m Keck I telescope in Hawaii in April and May 1998 using HIRES, the echelle spectrograph at the Nasmyth focus (Vogt et al. 1992). Data were collected for a total of 31 500 seconds with the cross disperser and echelle angles in a variety of settings so as to obtain almost complete wavelength coverage from 4400 to 9250 Å. A journal of the observations is presented in Table 1. The data were reduced with Tom Barlow’s HIRES reduction package (Barlow 1999, in preparation) which extracted sky-subtracted object spectra for each echelle order. The spectra were wavelength calibrated by reference to a Th-Ar hollow cathode lamp and mapped onto a linear, vacuum-heliocentric wavelength scale with a dispersion of 0.04 Å per wavelength bin. No absolute flux calibration was performed, although standard star spectra were obtained and are available (see §4 below). Lastly, the orders of the individual 2-D spectra and corresponding sigma error arrays were merged and then co-added with a weight proportional to their S/N.

The final spectrum has a resolution of 6 km s<sup>-1</sup> FWHM, sampled with  $\sim 3.5$  wavelength bins, and S/N between 30 and 150. The full spectrum is presented in Table 2, and in graphical format in Figure 1 (note that while this article and the corresponding PASP Research Note (paper version) presents only a small portion of the data, the spectrum in its entirety can be found in the electronic version of PASP). Given the exceptional quality of the data and the scope that they present for a wide range of research interests, we make them available to the astronomical community. Details of how to obtain additional material relating to this data are given in §4.

## 3. INTERVENING ABSORBERS IN THE SPECTRUM OF APM 08279+5255

### 3.1. The Ly $\alpha$ Forest

The rich forest of Ly $\alpha$  clouds, which is seen as a plethora of discrete absorption lines, is caused by line-of-sight passage through structures such as sheets and filaments in the intergalactic medium (IGM). Hydrodynamical simulations have shown that the Ly $\alpha$  forest

is a natural consequence of the growth of structure in the universe through hierarchical clustering in the presence of a UV ionizing background (e.g. Hernquist et al. 1996 ; Bi & Davidsen 1997). For a recent comprehensive review of the properties of the Ly $\alpha$  forest, see Rauch (1998).

We fitted Voigt profiles to the Ly $\alpha$  forest lines using the line fitting package VPFIT (Webb 1987) which determines the best fitting values of neutral hydrogen column density  $N(\text{H I})$ , absorption redshift,  $z_{\text{abs}}$ , and Doppler parameter  $b$  ( $= \sqrt{2}\sigma$ ) for each absorption component; the results are presented in Table 3. All Ly $\alpha$  lines within the redshift interval  $3.11 < z_{\text{abs}} < 3.70$  were fitted. The upper limit was chosen to avoid contamination of the sample by lines associated with ejected QSO material ( $z_{\text{abs}} = 3.70$  corresponds to the blue edge of the broad C IV absorption trough, at an ejection velocity of  $\sim 13\,000 \text{ km s}^{-1}$ ). The lower redshift limit,  $z_{\text{abs}} = 3.11$  in Ly $\alpha$ , corresponds to the onset of the Ly $\beta$  forest. Within these limits the line list in Table 3 is complete for column densities  $\log N(\text{H I}) > 12.5$ . However, we consider the values of  $N(\text{H I})$  to be accurate only for  $\log N(\text{H I}) < 14.5$  since the fits rely on the Ly $\alpha$  line alone which is saturated beyond this limit (no higher order Lyman lines were included in the solution because of the severe blending of the spectrum below the wavelength of Ly $\beta$  emission, even at the high resolution of the HIRES spectra).

The column density distribution in the Ly $\alpha$  forest can be represented by a power law of the form

$$n(N)dN = N_0 N^{-\beta} dN \quad (1)$$

(Rauch 1998 and references therein). The column density distribution for the present sample is reproduced in Figure 2. A maximum likelihood fit between  $12.5 < \log N(\text{H I}) < 15.5$  yields a power law index  $\beta = 1.27$  (Figure 3). This is likely to be a lower limit to true value of  $\beta$  because the line density of the forest at these redshifts is sufficiently high that lines can be missed due to blending. In other words, the spectra are confusion limited for weak Ly $\alpha$  lines. Hu et al. (1995) used simulations to model this effect and concluded that incompleteness sets in at  $\log N(\text{H I}) \simeq 13.20$  and that at the lowest column densities sampled,  $\log N(\text{H I}) = 12.30 - 12.60$ , only one in four Ly $\alpha$  clouds is detected. If we adopt the same incompleteness corrections as in Table 3 of Hu et al. (1995), we deduce  $\beta = 1.39$ , in good agreement with the value  $\beta = 1.46$  reported by these authors over a similar column density range as that considered here.

An analysis of the C IV  $\lambda\lambda 1548, 1550$  absorption associated with the Ly $\alpha$  forest has been presented elsewhere (Ellison et al. 1999). By fitting profiles to the observed C IV lines, Ellison et al. (1999) deduced a median  $N(\text{C IV})/N(\text{H I}) = 1.4 \times 10^{-3}$  for Ly $\alpha$  absorbers with  $\log N(\text{H I}) > 14.5$ . Of the 23 Ly $\alpha$  clouds within the redshift interval  $3.11 < z_{\text{abs}} < 3.70$  which exhibit associated C IV absorption, five also show Si IV  $\lambda\lambda 1393, 1402$  absorption; an

example is reproduced in Figure 4. Table 4 lists the parameters of the profile fits for these five absorption systems; the C IV and Si IV systems were fitted separately (that is, there was no attempt to force a common fit to both species). The values of the  $N(\text{Si IV})/N(\text{C IV})$  ratio deduced for the five systems ( $\log N(\text{Si IV})/N(\text{C IV}) \simeq -1.2$  to  $-0.1$ ) are typical of those found at these redshifts (Boksenberg, Sargent, & Rauch 1998).

### 3.2. Mg II Absorbers

The data presented here can be used to search for Mg II  $\lambda\lambda 2796, 2803$  systems at  $z_{\text{abs}} > 1$  with a higher sensitivity than achieved up to now, formally to a rest frame equivalent width detection limit of only a few mÅ. On the basis of the results by Churchill et al. (1999) we expect to find many Mg II systems in our spectrum and indeed a first pass has revealed nine systems between  $z_{\text{abs}} = 1.181$  and 2.066, which are reproduced in Figure 5. The rest frame equivalent widths of Mg II  $\lambda 2796$  span the range from  $W_r \simeq 2.5 \text{ \AA}$  ( $z_{\text{abs}} = 1.181$ ) to  $W_r = 11 \text{ m\AA}$  ( $z_{\text{abs}} = 1.688$ ). The former (see Figure 5a, top left-hand panel) is the most likely candidate for the lensing galaxy, given its strength and redshift. On the other hand, near  $z_{\text{abs}} = 1.55$  there is a complex of three closely spaced absorption systems, each in turn consisting of multiple components (Figure 5a, bottom panel); with a total velocity interval of  $\sim 450 \text{ km s}^{-1}$  such a configuration may arise in a galaxy cluster which presumably could also contribute to the lensing of the QSO.

Table 5 lists the absorption line parameters returned by VPFIT for five of the nine Mg II systems. We did not attempt to fit the  $z_{\text{abs}} = 1.181$  system because the lines are strongly saturated. Interestingly, for the other three systems—at  $z_{\text{abs}} = 1.211, 1.812,$  and  $2.041$ —VPFIT could not converge to a statistically acceptable solution, in the sense that there is no set of values of  $b$  and  $N(\text{Mg II})$  which can reproduce the observed profiles of *both* members of the doublet. The problem can be appreciated by considering, for example, the  $z_{\text{abs}} = 1.211$  system (Figure 5a, top right-hand panel). Here,  $\lambda 2796$  and  $\lambda 2803$  have approximately the same equivalent width, indicating that the lines are saturated and lie on the flat part of the curve of growth, and yet the residual intensity in the line cores is  $\approx 0.45$ .

We believe that the reason for this apparent puzzle lies in the gravitationally lensed nature of APM 08279+5255. Our spectrum is the superposition of two sight-lines separated by 0.35 arcsec and contributing in almost equal proportions to the total counts (Ledoux et al. 1998). If there are significant differences in the strength of Mg II absorption between the two sight-lines with—in the example considered here, saturated absorption along one and weak or no absorption along the other—the composite spectrum would have the character seen in our data.

Assuming the lens to be at  $z_{\text{lens}} = 1.181$  and an Einstein-de Sitter universe, the three absorption redshifts  $z_{\text{abs}} = 1.211, 1.812,$  and  $2.041$  correspond to transverse distances between the two sight-lines (at an angular separation of 0.35 arcseconds) of 1.5, 0.75 and  $0.59 h^{-1}$  kpc respectively. Some may be surprised to find large changes in the character of the absorption across such small distances, much smaller than the scales over which the overall kinematics of galactic halos vary (e.g. Weisheit & Collins 1976). In reality, micro-structure in low-ionization absorption lines is not unusual and has already been seen (even over sub-parsec scales) in the interstellar medium of the Milky Way (e.g. Lauroesch et al. 1998 and references therein), of the LMC (Spyromilio et al. 1995), and of the absorbing galaxy at  $z_{\text{abs}} = 3.538$  in front of another gravitationally lensed QSO, Q1422+231 (Rauch, Sargent, & Barlow 1999). These authors have recently reported *spatially resolved* HIRES observations of images A and C of this bright QSO, which are separated by 1.3 arcseconds.

While in our case it is not possible to deconvolve the individual contributions of the two sight-lines to our blended spectrum, because in general there is not a unique ‘solution’ to the composite Mg II absorption profiles, the data presented here provide a strong incentive to observe APM 08279+5255 spectroscopically with STIS on the *HST*. Our prediction is that Mg II absorption at  $z_{\text{abs}} = 1.211, 1.812,$  and  $2.041$  will exhibit significant differences between sight-lines A and B, and that such differences can be used to probe in fine detail the spatial structure of low ionization QSO absorbers, complementing the results of Rauch et al. (1999) on Q1422+231.

#### 4. Obtaining the data

The data presented in this paper are also available in electronic form at:

`ftp://ftp.ast.cam.ac.uk/pub/papers/APM08279`

As well as the quasar spectrum, which is presented in fits format with its associated error arrays, this site also contains standard star spectra (2-D), gzipped postscript plots of the complete QSO spectrum, an ascii file of a low resolution spectrum of APM 08279+5255 and a README file containing all other relevant information required for using these data. Any questions regarding the data can be addressed to SLE in the first instance.

We ask that any publications resulting from analyses of this spectrum fully acknowledge the W. M. Keck Observatory and Foundation with the standard pro forma, listed as a footnote on page 1, and reference this PASP Research Note as the source of the spectrum.

## 5. Summary

We have presented a brief analysis of the absorption systems seen in the HIRES echelle spectrum of the gravitationally lensed BAL QSO APM 08279+5255. The Ly $\alpha$  forest was analysed with Voigt profiles within a region ( $3.11 < z_{\text{abs}} < 3.70$ ) deemed to be free of contamination from higher order Lyman lines and ejected QSO material. The H I column density distribution is well fitted by a power law with slope  $\beta = 1.27$  between  $\log N(\text{H I}) = 12.5$  and  $15.5$ ; a higher value,  $\beta = 1.39$ , is obtained when allowance is made for line confusion at the low column density end of the distribution. Approximately half of the Ly $\alpha$  lines with  $\log N(\text{H I}) > 14.5$  have associated C IV absorption (Ellison et al. 1999); five of these C IV systems also show Si IV with ratios  $N(\text{Si IV})/N(\text{C IV})$  between  $\approx 1$  and  $\approx 1/15$ .

We identified nine Mg II systems between  $z_{\text{abs}} = 1.181$  and  $2.066$  two of which are candidates for absorption associated with the lens. For three Mg II systems we infer that there are spatial differences in the absorption between the light-paths to the two main images of the QSO (which are unresolved in our study). Given the exceptional brightness of APM 08279+5255, the spectrum presented here is among the best ever obtained for a high redshift QSO; we make it available to the astronomical community so that it can be used in conjunction with other forthcoming studies of this remarkable object and sightline.

## REFERENCES

- Bi, H. & Davidsen, A. F. 1997, *ApJ*, 479, 523
- Boksenberg, A., Sargent, W.L.W., & Rauch, M. 1998, in *The Birth of Galaxies*, eds. B. Guiderdoni, F.R. Bouchet, Trinh X. Thuan, & Tran Thanh Van (Gif-sur-Yvette: Editions Frontieres), in press (astro-ph/9810502)
- Churchill, C. W., Rigby, J. R., Charlton, J. C., & Vogt, S. S. 1999, *ApJS*, 120, 51
- Downes, D., Neri, R., Wilkind, T., Wilner, D. J., & Shaver, P. 1999, *ApJ*, 513, L1
- Ellison, S. L., Lewis, G. F., Pettini, M., Chaffee, F. H. & Irwin, M. J. 1999, *ApJ*, in press (astro-ph/9903063)
- Hernquist, L., Katz, N., Weinberg, D. H., & Miralda-Escudé, J. 1996, *ApJ*, 457, L51
- Hines, D. C., Schmidt, G. D. & Smith, P. S. 1999, *ApJ*, 514, L91
- Hu, E.M., Kim, T-S., Cowie, L.L., Songaila, A., & Rauch, M. 1995, *AJ*, 110, 1526
- Ibata, R. A., Lewis, G. F., Irwin, M. J., Lehár, J. & Totten, E. J. 1999, in preparation
- Irwin, M. J., Ibata, R. A., Lewis, G. F., & Totten, E. J. 1998, *ApJ*, 505, 529
- Lauroesch, J.T., Meyer, D.M., Watson, J.K., & Blades, J.C. 1998, *ApJ*, 507, L89
- Ledoux, C., Theodore, B., Petitjean, P., Bremer, M. N., Lewis, G. F., Ibata, R. A., Irwin, M. J., & Totten, E. 1998, *A&A*, 339, L77
- Lewis, G. F., Chapman, S. C., Ibata, R. A., Irwin, M. J. & Totten, E. J. 1998, *ApJ*, 505, L1
- Rauch, M. 1998, *ARA&A*, 36, 267
- Rauch, M., Sargent, W.L.W., & Barlow, T.A. 1999, *ApJ*, in press (astro-ph/9812027)
- Spyromilio, J., Malin, D.F., Allen, D.A., Steer, C.J., & Couch, W.J. 1995, *MNRAS*, 274, 256
- Vogt, S. S. 1992, in *ESO Conf. and Workshop Proc 40, High Resolution Spectroscopy with the VLT*, ed. M.-H. Ulrich (Garching: ESO), 223
- Webb J. K. 1987, PhD thesis, University of Cambridge
- Weisheit, J. C., & Collins, L. A. 1976, *ApJ*, 210, 299





Table 1. JOURNAL OF HIRES OBSERVATIONS OF APM 08279+5255

Date	Integration time (s)	Wavelength range (Å)	Typical S/N
April 1998	1800	4400 – 5945	15
April 1998	1800	4400 – 5945	15
April 1998	1800	4400 – 5945	15
April 1998	1800	4400 – 5945	15
May 1998	2700	4410 – 5950	25
May 1998	2700	4400 – 5945	25
May 1998	900	5440 – 7900	30
May 1998	3000	5440 – 7900	60
May 1998	3000	5440 – 7900	60
May 1998	3000	5475 – 7830	55
May 1998	3000	5475 – 7830	55
May 1998	3000	6765 – 9150	50
May 1998	3000	6850 – 9250	50
Summed Total	31 500	4400 – 9250	30 –150

Table 2. ASCII LISTING OF THE HIRES SPECTRUM OF  
APM 08279+5255 SHOWN IN FIGURE 1 <sup>a</sup>

Wavelength (Å)	Data (counts)	1 $\sigma$ error
5700.00	337.59	7.29
5700.04	319.87	7.13
5700.08	296.68	6.93
5700.12	281.57	6.77
5700.16	265.92	6.66
5700.20	246.77	6.45
5700.24	233.27	6.34
5700.28	238.33	6.39
5700.32	217.76	6.19
5700.36	219.35	6.19

<sup>a</sup>The full version of the Table is available in the electronic version of the PASP Research Note; only the first 10 lines are reproduced in this printed version.

Table 3. VOIGT PROFILE PARAMETER FITS FOR Ly $\alpha$  LINES WITH  
 $\log N(\text{H I}) > 12.5$  AND  $3.11 < z_{\text{abs}} < 3.70$ <sup>a</sup>

Redshift, $z_{\text{abs}}^b$	$\log N(\text{H I})^c$	$b$ value (km s <sup>-1</sup> ) <sup>d</sup>
3.14990	13.51 <sup>3</sup>	24.8 <sup>1</sup>
3.15073	12.75 <sup>3</sup>	12.2
3.15109	12.55 <sup>3</sup>	36.5 <sup>3</sup>
3.15366	13.93	42.0
3.15465	13.35	36.0
3.15637	12.95	16.5
3.15741	12.70	7.0 <sup>1</sup>
3.15783	12.92 <sup>3</sup>	7.6 <sup>1</sup>
3.15840	14.10	33.1
3.15930	14.43	20.9

<sup>a</sup>The full version of the Table is available in the electronic version of the PASP Research Note; only the first 10 lines are reproduced in this printed version. The error designations below also apply to the flags in the full version of this table.

<sup>b</sup>Redshift error =  $\pm 10^{-5}$

<sup>c</sup> $N(\text{HI})$  error < 30% unless otherwise stated

<sup>d</sup>Doppler parameter error < 10% unless otherwise stated

<sup>1</sup>Error < 20%

<sup>2</sup>Error < 30%

<sup>3</sup>Error > 30%

Table 4. VOIGT PROFILE FITS FOR METAL LINE SYSTEMS THAT EXHIBIT BOTH C IV AND Si IV ABSORPTION

Transition, X	Redshift, $z_{\text{abs}}^a$	$\log N(X)^b$	$b$ value (km s $^{-1}$ ) <sup>c</sup>
C IV	3.37677	12.24	24.5
C IV	3.37757	12.81	6.5
C IV	3.37770	13.28	19.7
C IV	3.37882	12.37	10.8
C IV	3.37891	13.24	22.5
C IV	3.37969	13.56	45.4
C IV	3.37969	12.89	17.0
Total C IV		13.96±0.03	
Si IV	3.37857	12.36	6.6
Si IV	3.37881	12.77	9.2
Si IV	3.37907	12.44	10.9
Si IV	3.37948	12.21	12.8
Si IV	3.37979	12.52	37.5
Si IV	3.37982	11.95	7.7
Si IV	3.38027	11.41	3.1
Total Si IV		13.23±0.02	
C IV	3.50125	13.01	16.8
C IV	3.50141	12.39	9.9
C IV	3.50204	12.24	5.3
C IV	3.50209	13.08	22.6
C IV	3.50281	12.39	32.8
Total C IV		13.46±0.04	
Si IV	3.50123	12.55	14.9
Si IV	3.50131	12.14	2.7
Si IV	3.50146	12.35	6.7
Si IV	3.50198	12.90	10.1
Si IV	3.50219	12.29	7.6
Si IV	3.50237	12.71	9.9
Total Si IV		13.35±0.02	

Table 4—Continued

Transition, X	Redshift, $z_{\text{abs}}^a$	$\log N(X)^b$	$b$ value (km s $^{-1}$ ) <sup>c</sup>
C IV	3.51380	12.88	17.1
C IV	3.51436	12.54	14.8
Total C IV		13.04 ±0.03	
Si IV	3.51341	11.71	1.4
Si IV	3.51357	11.65	3.3
Si IV	3.51376	12.58	9.3
Si IV	3.51401	12.02	4.6
Si IV	3.51423	11.62	5.6
Total Si IV		12.79±0.03	
C IV	3.55811	12.85	11.5
C IV	3.55842	12.63	12.7
Total C IV		13.06±0.03	
Si IV	3.55826	11.82	14.4
Total Si IV		11.82±0.10	
C IV	3.66863	12.88	89.3
C IV	3.66892	13.22	36.9
C IV	3.67082	12.97	21.4
C IV	3.67131	12.81	15.3
Total C IV		13.60 ±0.08	
Si IV	3.67022	12.22	8.0
Si IV	3.67076	12.36	9.8
Total Si IV		12.60±0.05	

<sup>a</sup>Redshift error = ±10 $^{-5}$

<sup>b</sup>Column density error < 40% for individual components. Total error for each metal line system indicated individually

<sup>c</sup>Doppler parameter error < 15%

Table 5. VOIGT PROFILE PARAMETER FITS TO Mg II SYSTEMS

Redshift, $z_{abs}^a$	$\log N(\text{Mg II})^b$	$b$ value ( $\text{km s}^{-1}$ ) <sup>c</sup>
1.29083	11.98	3.8
1.29101	11.58	11.6
Total Mg II	$12.13 \pm 0.05$	
1.44442	11.73	3.2
1.44433	11.87	13.9
Total Mg II	$12.11 \pm 0.12$	
1.54859	11.80	8.6
Total Mg II	$11.80 \pm 0.15$	
1.54949	11.55	2.2
1.54996	12.31	4.9
1.54959	12.04	4.3
1.54973	12.44	10.5
1.55000	11.86	15.0
Total Mg II	$12.84 \pm 0.03$	
1.55226	12.26	5.2
1.55238	12.21	4.2
Total Mg II	$12.54 \pm 0.02$	
1.68727	11.47	8.3
Total Mg II	$11.47 \pm 0.20$	
2.06685	12.40	29.4
2.06784	11.65	21.3
2.06669	11.75	4.6
Total Mg II	$12.55 \pm 0.04$	

<sup>a</sup>Redshift error =  $\pm 10^{-5}$

<sup>b</sup>Column density error < 40% for individual components. Total error for each metal line system indicated individually

<sup>c</sup>Doppler parameter error < 15%

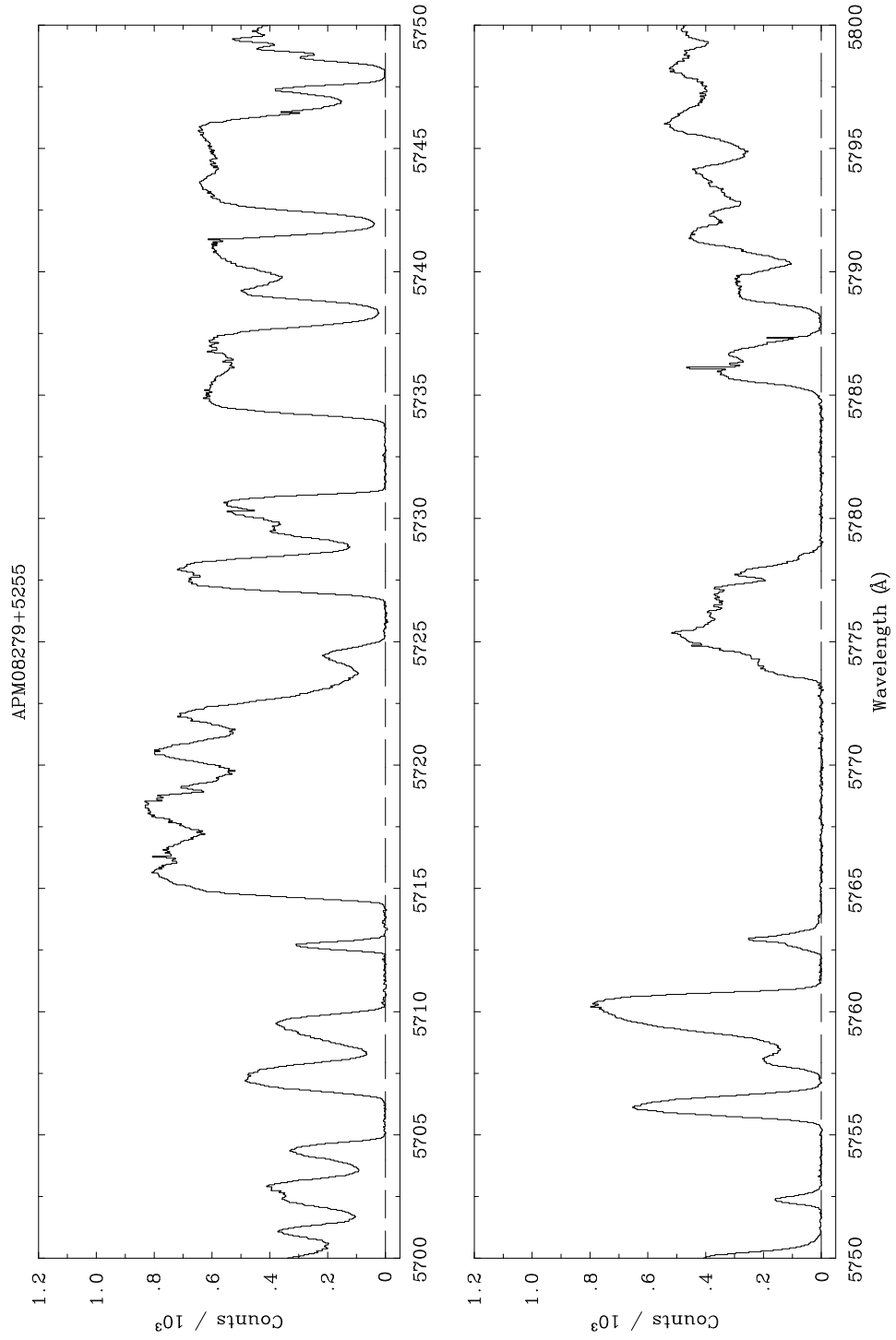


Fig. 1.— A 100 Å section of the HIRES spectrum of APM 08279+5255, between 5700 and 5800Å.



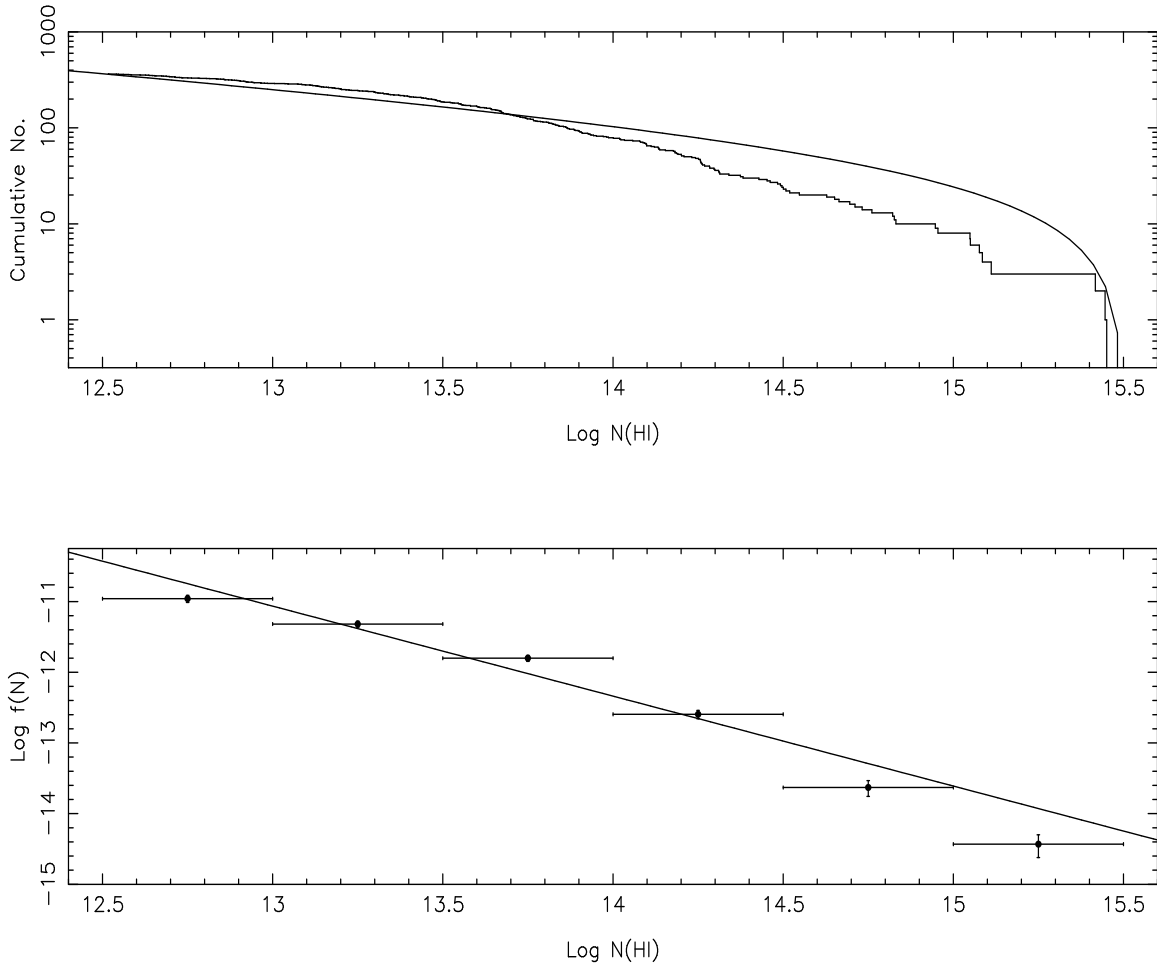


Fig. 2.— The column density distribution function for the Ly $\alpha$  forest in APM 08279+5255, in cumulative (top) and differential (bottom) forms. The data have been binned for display purposes only. In each panel the continuous line refers to a power law distribution with exponent  $\beta = 1.27$  (see Figure 3).

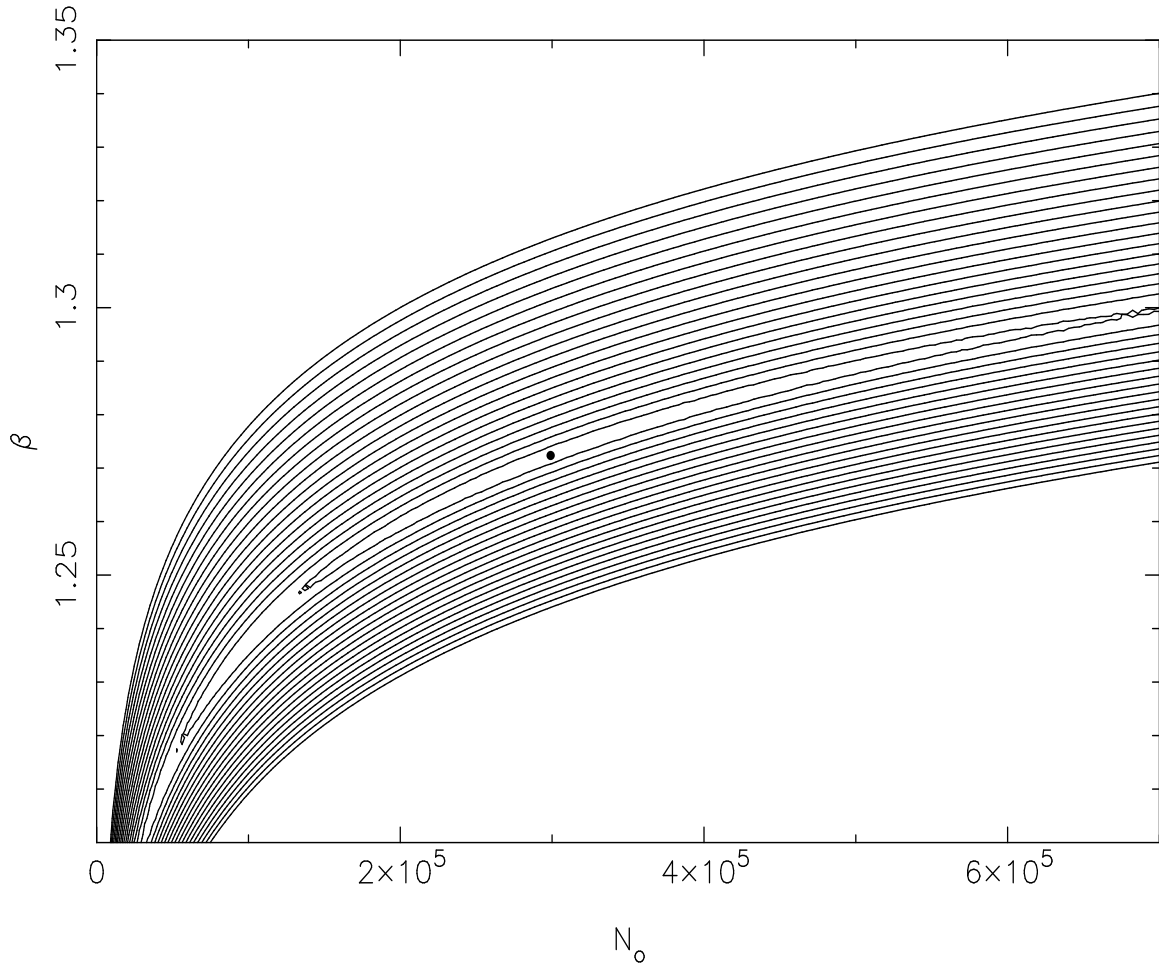


Fig. 3.— Maximum likelihood contours for the fit to the  $N(\text{H I})$  column density distribution assuming a power law of the form given in eq. (1).

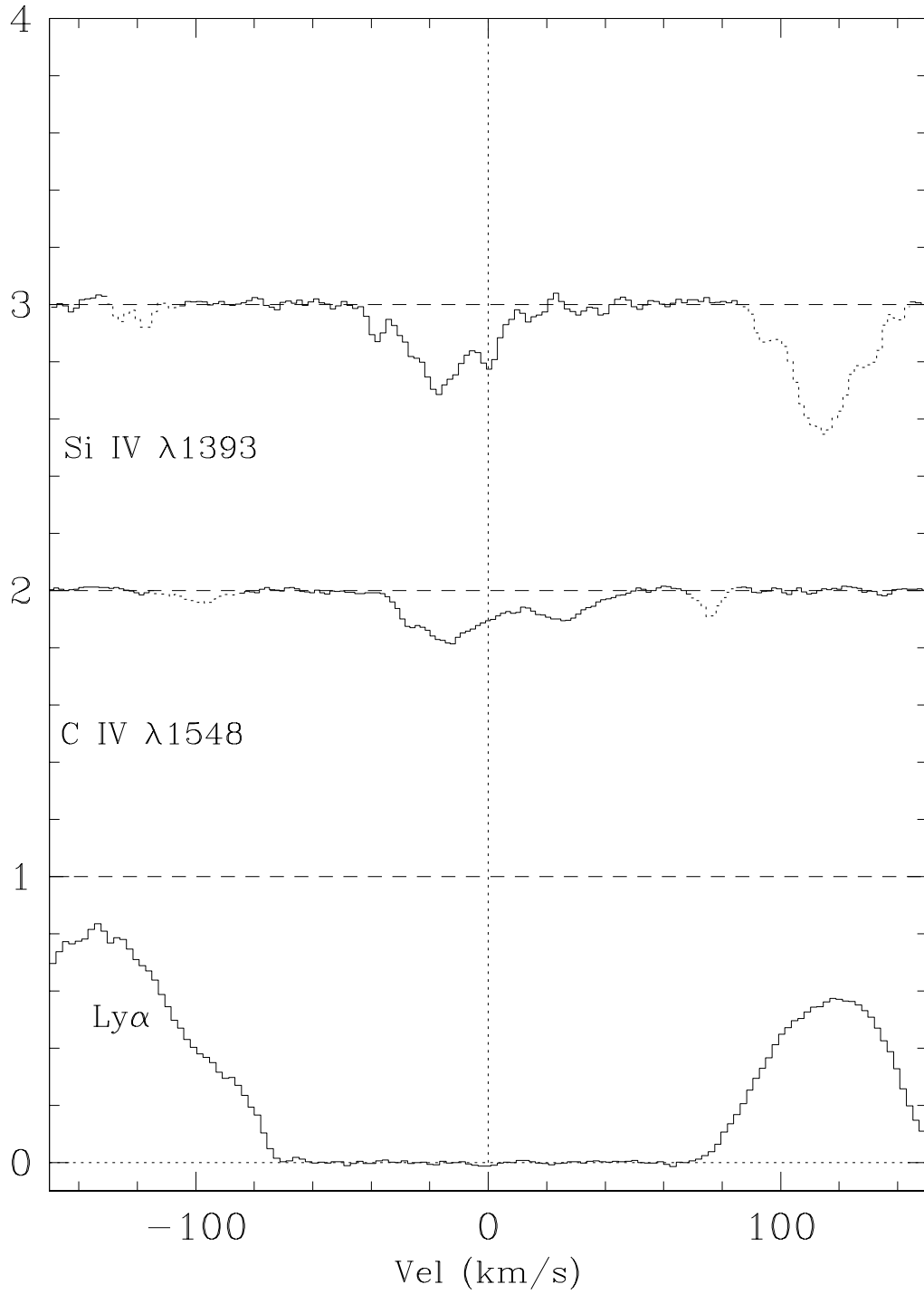


Fig. 4.— An example of a saturated Ly $\alpha$  line with associated C IV and Si IV absorption (the scale of the y-axis has been offset for clarity). This is the absorption system at  $z_{\text{abs}} = 3.514$  in Table 4, with  $\log N(\text{C IV}) = 13.04$  and  $\log N(\text{Si IV}) = 12.79$  (absorption features from other systems are shown with broken lines).

